

**$\beta$  decay spectroscopy of light Nd isotopes**E. A. McCutchan,<sup>1,2</sup> R. F. Casten,<sup>1</sup> V. Werner,<sup>1</sup> R. J. Casperson,<sup>1</sup> A. Heinz,<sup>1</sup> J. Qian,<sup>1</sup>  
B. Shoraka,<sup>1,3</sup> J. R. Terry,<sup>1</sup> E. Williams,<sup>1</sup> and R. Winkler<sup>1</sup><sup>1</sup>Wright Nuclear Structure Laboratory, Yale University, New Haven, Connecticut 06520, USA<sup>2</sup>National Nuclear Data Center, Brookhaven National Laboratory, Upton, New York 11973, USA<sup>3</sup>University of Surrey, Guildford, Surrey GU2 7XH, United Kingdom

(Received 5 April 2013; published 28 May 2013)

Excited states in  $^{132,134}\text{Nd}$  were populated in the  $\beta^+/\epsilon$  decay of  $^{132,134}\text{Pm}$  and studied through off-beam  $\gamma$ -ray spectroscopy. Level spins and multipole mixing ratios of transitions were determined through an angular correlation analysis. In  $^{132}\text{Nd}$ , a new excited  $0^+$  state is identified and in  $^{134}\text{Nd}$  the level scheme is significantly extended. Differences in the location of the  $0^+$  state and the  $\gamma$  bandhead above and below  $N = 82$  suggest that the lighter isotopes are much more  $\gamma$ -soft than the heavier Nd and that a first-order phase transitional description is not applicable in the  $N < 82$  region.

DOI: [10.1103/PhysRevC.87.057306](https://doi.org/10.1103/PhysRevC.87.057306)

PACS number(s): 23.40.-s, 21.10.Re, 21.60.Ev, 27.60.+j

In the rare-earth region for nuclei around  $N = 90$ , there has been considerable discussion concerning the structural interpretation. Interest in this region blossomed with the concept that the  $N = 90$  nuclei exhibited a specific type of phase transitional behavior [1–4] described by the X(5) model [5]. In subsequent works [6–8] alternative interpretations involving more generalized shape coexistence models have been argued. Regardless of the origin of the observed properties, it is clear that the  $N = 90$  nuclei exhibit an intriguing and unique structure. An interesting question is whether or not such features are exhibited by nuclei below  $N = 82$ . The  $N < 82$  region has significantly less known information on nonyrast levels, due to the difficulty in populating these states with the heavy-ion reactions needed to produce such highly proton-rich nuclei. Based on yrast band energies, the light Nd and Sm nuclei have been proposed [9] to exhibit a structure similar to an axially symmetric deformed rotor. Later lifetime measurements [10] demonstrated that it was difficult to distinguish between an axially symmetric or  $\gamma$ -soft deformed potential based on yrast band properties alone. A more recent work [11], focusing on the search for phase transitional behavior in  $^{130}\text{Ce}$ , revealed substantial disagreements from an X(5) description, possibly originating from a soft-potential in the  $\gamma$  degree of freedom.

The purpose of this Brief Report is to explore the proton-rich Nd nuclei in the region where phase transitional behavior can be investigated. The  $N = 90$  neodymium isotope is  $^{150}\text{Nd}$  with eight valence neutrons. Consequently, the analogous isotope below  $N = 82$  is  $^{134}\text{Nd}$ . It is well known [9] that the onset of deformation is more gradual for the  $N < 82$  isotopes compared with those above  $N = 82$ . To determine what similarities exist, if any, with their  $N > 82$  counterparts,  $\beta$  decay was used to populate nonyrast states in  $^{132}\text{Nd}$  and  $^{134}\text{Nd}$ .

The parent nuclei were produced by bombarding a  $\sim 4$  mg/cm<sup>2</sup>  $^{92}\text{Mo}$  target with a 1-pnA, 230-MeV  $^{46}\text{Ti}$  beam provided by the Yale ESTU tandem accelerator. The target was backed by a 10 mg/cm<sup>2</sup> Au foil to stop all recoiling nuclei. The experiment was performed with a beam-on/beam-off cycle of 10-s intervals. In the beam-off cycle,  $\gamma$  rays were detected

using eight Compton-suppressed clover HPGe detectors. Both  $\gamma$ -ray singles (5 h) and  $\gamma$ - $\gamma$  coincidence (70 h) data were acquired. The energy range covered  $\sim 40$  to 2000 keV. The experiment yielded  $3.5 \times 10^8$  clover-clover coincidence events and  $6.1 \times 10^6$  clover singles events. The beam energy was chosen to optimize the yield of  $^{132,134}\text{Pm}$  via the  $3p3n$  and  $3pn$  reaction channels, respectively. Many additional isotopes were produced either directly as evaporation residues or through  $\beta$  decay. The strong reaction channels can be seen in Fig. 1(a), which gives the total projection of the  $\gamma$ - $\gamma$  matrix. The quality of the coincidence data is illustrated in Fig. 1(b) with a gate on the 294-keV  $2_1^+ \rightarrow 0_1^+$  transition in  $^{134}\text{Nd}$ .

The array consisted of detector pairs at relative angles of  $56^\circ$ ,  $97^\circ$ , and  $180^\circ$ . In addition to a summed  $\gamma$ - $\gamma$  matrix of all clover data, used to construct the level schemes and determine intensities of transitions, matrices were also constructed by sorting on detector pairs for angular correlation analysis. The ratios  $W_a = W(97^\circ)/W(180^\circ)$  and  $W_b = W(97^\circ)/W(56^\circ)$  were used to determine  $J$  assignments and deduce multipole mixing ratios,  $\delta$ , following the procedure described in Ref. [12].

The evaluated  $\beta$  decay data [13] on  $^{132}\text{Nd}$  are based on a single  $\beta$  decay study, reported initially in Ref. [14] and more completely in Ref. [15]. The parent  $^{132}\text{Pm}$  nuclei decay with  $T_{1/2} = 6.3$  s from a  $J^\pi = (3^+)$  ground state. The spin assignment is based [13] solely on the  $J^\pi$  of the levels observed to be directly populated in  $\beta$  decay. Note that the neighboring odd-odd nuclei undergo  $\beta$  decay from ground and isomeric states with a wide range of  $J^\pi$  values.  $^{134}\text{Pm}$  decays via a  $(2^+)$  ground state and a  $(5^+)$  isomer [16] and  $^{130}\text{Pr}$  decays via three states [17] with  $J = 2^+$ ,  $(4,5)^+$ , and  $(7,8)$ . It is possible that  $^{132}\text{Pm}$  also possesses two  $\beta$ -decaying states, which would be consistent with a wide range of spins in  $^{132}\text{Nd}$  being populated in the decay.

Table I lists the levels populated in  $^{132}\text{Nd}$  and their  $\gamma$  decay. The present level scheme is given in Fig. 2(a). Four new levels are established and no evidence is found for the 1388-keV level previously proposed [15]. Angular correlation measurements provided firm spin assignments for two previously observed and one newly identified level.

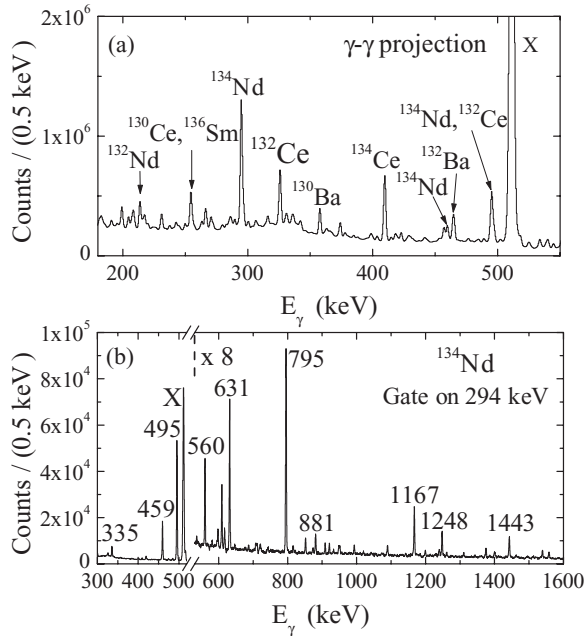


FIG. 1. (a) Projection of the  $\gamma$ - $\gamma$  matrix. Strong peaks observed in the beam-off interval are labeled by the  $\beta$  decay daughter nucleus. (b) Clover-clover coincidence spectrum gated on the 294-keV  $2_1^+ \rightarrow 0_1^+$  transition in  $^{134}\text{Nd}$ . Intense transitions belonging to  $^{134}\text{Nd}$  are labeled by their energy in keV. The  $y$  scale in (b) is multiplied by 8 for  $E_\gamma > 520$  keV. The 511-keV annihilation line is indicated by an X.

A level at 823 keV is reported [13] to decay to the  $2_1^+$  and  $0_1^+$  states and is tentatively assigned a  $J^\pi$  of  $2^+$ . In the present work, angular correlation analysis of the 610-keV  $2_2^+ \rightarrow 2_1^+$  transition confirms the previous spin assignment and indicates that the transition is mainly  $E2$ , with  $\delta < -10$ . The 823-keV  $2_2^+ \rightarrow 0_1^+$  transition could not be confirmed in the present

TABLE I. Levels populated in  $^{132}\text{Nd}$  and their  $\gamma$  decay.  $I_\gamma$  gives the intensity in  $\beta$  decay normalized to the 213-keV  $2_1^+ \rightarrow 0_1^+$  transition. The angular correlation ratios,  $W_a = W(97^\circ)/W(180^\circ)$  and  $W_b = W(97^\circ)/W(56^\circ)$ , were used to determine the mixing ratio  $\delta$  of the transition.

$J_i^\pi$	$E_i$ (keV)	$E_\gamma$ (keV)	$I_\gamma$	$W_a$	$W_b$	$\delta$
$2^+$	213.09(5)	213.09(5)	100(10)			
$4^+$	610.92(6)	397.83(5)	8.1(6)			
$2^+{}^a$	823.38(7)	610.29(6)	5.4(4)	1.07(8)	1.21(7)	$< -10$
$0^+{}^a$	873.87(8) <sup>b</sup>	660.78(6) <sup>c</sup>	2.2(2)	0.39(4)	1.50(13)	$E2$
	1031.52(9) <sup>b</sup>	818.41(8) <sup>c</sup>	1.0(1)			
		420.62(8) <sup>c</sup>	0.43(6)			
$3^+{}^a$	1117.36(9)	904.27(8)	2.6(3)	1.38(15)	0.99(8)	$< -8$
	1223.6(1) <sup>b</sup>	612.67(10) <sup>c</sup>	1.1(2)			
	1703.6(1) <sup>b</sup>	1490.6(1) <sup>c</sup>	1.2(2)			
		1092.7(1) <sup>c</sup>	0.8(2)			

<sup>a</sup>Spin assignment from angular correlation analysis.

<sup>b</sup>Level was not previously reported.

<sup>c</sup> $\gamma$ -ray line was not previously reported.

study due to the presence of a very strong 822-keV transition originating from  $^{132}\text{Ce}$  [13].

A new level at 873.9 keV is identified in the present work based on a strong, single depopulating transition of 660.8 keV to the  $2_1^+$  state. In the  $\gamma$ - $\gamma$  angle matrices gated on the 213-keV  $2_1^+ \rightarrow 0_1^+$  transition, most transitions show small variation in relative intensities, whereas the relative intensity of the 661-keV transition is significantly enhanced in the  $180^\circ$  detector group, as shown in Fig. 3. This enhancement is a feature of only a  $0-2-0$  cascade and a full analysis of the angular correlation data supports a spin assignment of  $0^+$  for the 874-keV level.

A level at 1117 keV was established in  $\beta$  decay [13] based on a transition to the  $2_1^+$  state and tentatively assigned  $J^\pi = 3^+$ . The angular correlation of the 904-keV  $3_1^+ \rightarrow 2_1^+$  transition confirms the  $J = 3$  assignment and indicates that the multipolarity is nearly pure  $E2$ . In Ref. [15] a 294-keV depopulating transition to the  $2_2^+$  state was tentatively placed, with the uncertainty arising from the presence of the very strong 294-keV transition in  $^{134}\text{Nd}$ . Our experiment faces the same difficulty and thus we can make no definite conclusion about a 294-keV  $3_1^+ \rightarrow 2_2^+$  transition in  $^{132}\text{Nd}$ .

The  $\beta$  decay studies of  $^{134}\text{Nd}$  include Refs. [14,15,18], with the adopted data [16] based mainly on Ref. [18]. The decay of  $^{134}\text{Pm}$  occurs through the ( $2^+$ ) ground state ( $T_{1/2} \sim 5$  s) and a ( $5^+$ ) isomer ( $T_{1/2} \sim 22$  s). Table II lists the levels populated in  $^{134}\text{Nd}$  and their  $\gamma$  decay. The present level scheme for levels populated below 2000 keV is given in Fig. 2(b). Ten new levels are established in the present work and the decay properties of several levels are revised (see Table II).

A level at 754 keV was reported in  $\beta$  decay [16] based on transitions to the  $2_1^+$  and  $0_1^+$  states and tentatively assigned a  $J^\pi$  of  $2^+$ . We confirm the two depopulating transitions, but we find some discrepancy with the reported [16] intensities, indicated in Table II. The current branching ratio from the 754-keV level was measured in several different gates on transitions populating the level; each spectrum consistently gave a smaller intensity for the 754-keV  $\gamma$  ray compared with the 459-keV  $\gamma$ -ray. Angular correlation analysis of the 459–294 cascade yielded  $W_a = 1.01(4)$  and  $W_b = 1.27(4)$ , which are consistent with  $J = 2$  for the level and  $\delta < -15$  for the 459-keV transition.

A level at 1089 keV was reported [16] on the basis of two depopulating transitions to the  $2_2^+$  and  $2_1^+$  levels; these are confirmed in the present work. An additional transition of 299.9 keV to the  $4_1^+$  level is newly identified. The 1089-keV level was tentatively assigned  $J^\pi = 3^+$  and proposed as a quasi- $\gamma$  band member [16]. From the angular correlation analysis,  $W_a = 0.995(36)$  and  $W_b = 0.948(22)$  is obtained for the 795-keV transition and  $W_a = 1.40(12)$  and  $W_b = 1.07(8)$  is obtained for the 335-keV transition. This confirms the  $J = 3$  assignment to the level and gives  $\delta = -3_{+1}^{-2}$  for the 795-keV transition and two possible mixing ratios,  $\delta < -25$  or  $\delta = 0.25(2)$ , for the 335-keV transition.

Figure 4 compares the low-lying states of  $^{132}\text{Nd}$  to those in the isotone  $^{130}\text{Ce}$  and the  $N = 90$  nucleus  $^{150}\text{Nd}$ . The  $R_{4/2} = E(4_1^+)/E(2_1^+)$  values are very similar: 2.80, 2.87, and 2.93 for  $^{130}\text{Ce}$ ,  $^{132}\text{Nd}$  and  $^{150}\text{Nd}$ , respectively; all are close to the X(5) value of 2.91. Note that the  $R_{4/2}$  value of  $^{134}\text{Nd}$  is

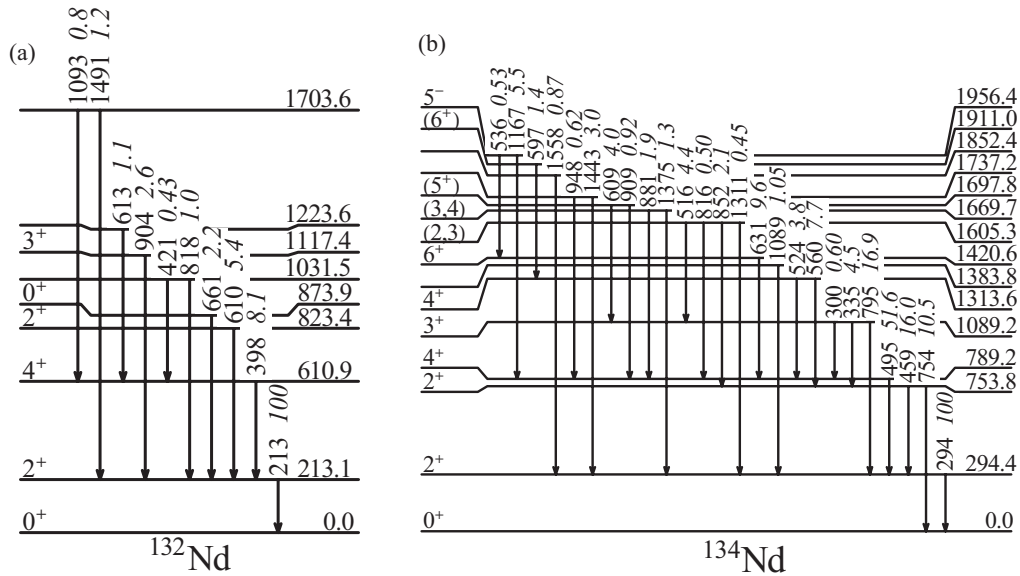


FIG. 2. Partial level schemes of (a)  $^{132}\text{Nd}$  and (b)  $^{134}\text{Nd}$  populated in the  $\beta^+/\epsilon$  decay of  $^{132}\text{Pm}$  and  $^{134}\text{Pm}$ , respectively. Levels are labeled by their energy in keV.  $\gamma$ -ray transitions are labeled by their energy in keV and relative intensities (in italics), normalized to the  $2_1^+ \rightarrow 0_1^+$  transition in each nucleus. For  $^{134}\text{Nd}$ , only levels up to 2 MeV are presented.

2.68, reflecting the more gradual onset of collectivity below compared with above  $N = 82$ , where  $R_{4/2}$  changes more abruptly from 2.49 in  $^{148}\text{Nd}$ . A near degeneracy of the  $0_2^+$  state with the  $6^+$  member of the yrast band is taken as a signature of the X(5) model. From Fig. 4, it is clear that such a feature is exhibited by  $^{150}\text{Nd}$ . In the  $N = 72$  isotones, however, the  $0_2^+$  level in  $^{130}\text{Ce}$  and the new  $0_2^+$  level in  $^{132}\text{Nd}$  are depressed, relative to the  $6^+$  state, suggesting basic structural differences compared with the  $N > 82$  neodymium isotopes.

Furthermore, one can see that the location of the  $\gamma$  band differs significantly when comparing the isotopes above and below  $N = 82$ . In  $^{150}\text{Nd}$ , the  $\gamma$  band lies quite high in excitation energy, with  $R_{2\gamma} = E(2_2^+)/E(2_1^+) = 8.2$ . This is consistent with the concept underlying the X(5) model, which takes an axially symmetric potential in  $\gamma$  centered around  $\gamma = 0$ . The  $N = 72$  isotones of both Nd and Ce, however, have  $R_{2\gamma}$  values between 3 and 4, which indicates considerable  $\gamma$ -softness in their potential. Based on the energies of the two basic nonyrast levels,  $0_2^+$  and  $2_2^+$ , X(5) behavior in this region below  $N = 82$  can be ruled out.

In conclusion, levels in  $^{132}\text{Nd}$  and  $^{134}\text{Nd}$  have been studied following their population in  $\beta^+/\epsilon$  decay. In  $^{132}\text{Nd}$ , a new excited  $0^+$  level is identified and in  $^{134}\text{Nd}$  the level scheme is extended. The yrast band levels of  $^{132}\text{Nd}$  are similar to those of the  $N = 90$  nucleus  $^{150}\text{Nd}$  and to the predictions of the X(5) model. However, the newly identified first excited  $0^+$  level and the firmly identified  $2^+$   $\gamma$  bandhead are found to be lower in energy compared with  $^{150}\text{Nd}$  and the X(5) model, pointing to

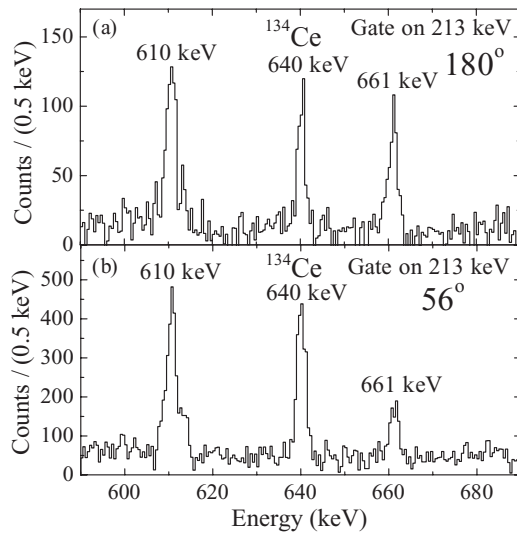


FIG. 3. Evidence for an excited  $0^+$  state in  $^{132}\text{Nd}$ . Spectra are gated on the 213-keV  $2_1^+ \rightarrow 0_1^+$  transition showing the relative intensities of the 610- and 661-keV transitions in the (a)  $180^\circ$  and (b)  $56^\circ$  detector groups. The 610-keV transition results from a  $2-2-0$  cascade, while the 640-keV transition in  $^{134}\text{Ce}$  is from a  $5-4-(4)-2$  cascade.

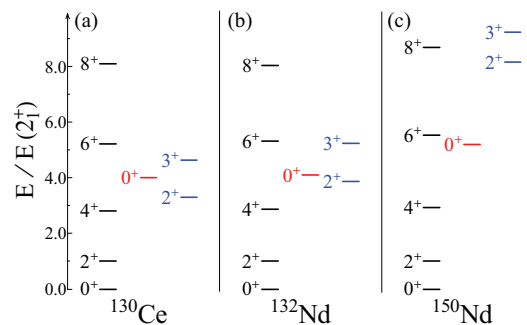


FIG. 4. (Color online) Comparison of low-lying levels in (a)  $^{130}\text{Ce}$ , (b)  $^{132}\text{Nd}$ , and (c)  $^{150}\text{Nd}$ . Energies are normalized to the first  $2_1^+$  level energy in each nucleus.

TABLE II. Levels populated in  $^{134}\text{Nd}$  and their  $\gamma$  decay.  $I_\gamma$  gives the intensity in  $\beta$  decay normalized to the 294-keV  $2_1^+ \rightarrow 0_1^+$  transition, while  $B$  gives the relative intensity from each level, normalized to the strongest branch.

$J_i^\pi$	$E_i$ (keV)	$E_\gamma$ (keV)	$I_\gamma$	$B$	$B_{lit}^a$
$2^+$	294.36(5)	294.36(5)	100(5)	100(5)	100(5)
$2^{+b}$	753.78(6)	753.81(6)	10.5(5)	66(3)	111
		459.39(5)	16.0(10)	100(6)	100
$4^+$	789.24(6)	494.88(5)	51.6(26)	100(5)	100
$3^{+b}$	1089.16(5)	794.83(6)	16.9(12)	100(7)	100(12)
		335.38(7)	4.5(3)	27(2)	29(9)
		299.9(1) <sup>c</sup>	0.60(10)	3.6(6)	
$4^{+b}$	1313.56(8)	[1019]	<0.3	<4	
		559.76(8)	7.7(6)	100(8)	100(8)
		524.34(9)	3.8(3)	49(4)	65(8)
	1383.78(9) <sup>d</sup>	1089.42(8) <sup>c</sup>	1.05(12)	100(11)	
$6^+$	1420.56(7)	631.32(6)	9.6(7)	100(7)	100
$(2,3)^b$	1605.28(8)	1310.9(1) <sup>c</sup>	0.45(5)	10.2(11)	
		851.53(8)	2.1(1)	48(2)	34(7)
		816.0(1) <sup>c</sup>	0.50(8)	11.4(18)	
		516.11(9)	4.4(3)	100(7)	100(14)
$(3,4)^b$	1669.71(9) <sup>e</sup>	1375.3(1) <sup>c</sup>	1.3(2)	68(10)	
		880.51(7)	1.9(2)	100(11)	
$(5^+)$	1697.79(9)	908.6(1) <sup>c</sup>	0.92(7)	23(2)	
		608.60(8)	4.0(2)	100(5)	100
	1737.21(9) <sup>f</sup>	1442.8(1) <sup>g</sup>	3.0(2)	100(7)	
		947.97(8) <sup>c</sup>	0.62(6)	21(2)	
	1852.4(1) <sup>f</sup>	1558.1(1) <sup>c</sup>	0.87(9)	100(10)	
$(6^+)$	1910.97(9)	597.41(8)	1.4(2)	100(14)	100(10)
$(5^-)$	1956.4(1)	1167.19(9)	5.5(4)	100(7)	100
		535.8(1) <sup>c</sup>	0.53(5)	9.6(9)	
	2036.85(10)	1247.6(1)	3.0(2)	100(7)	100
	2086.3(1) <sup>f</sup>	1791.9(1) <sup>c</sup>	1.0(1)	100(10)	
	2106.8(1) <sup>f</sup>	793.2(1) <sup>c</sup>	0.37(5)	100(14)	
		686.27(9) <sup>c</sup>	0.31(5)	84(14)	
	2328.96(13) <sup>f</sup>	1539.7(1) <sup>c</sup>	0.65(8)	81(10)	
		1239.8(1) <sup>c</sup>	0.80(8)	100(10)	
	2413.57(9) <sup>f</sup>	993.01(8) <sup>c</sup>	0.97(11)	100(11)	
	2430.6(1) <sup>f</sup>	1641.5(2) <sup>c</sup>	0.77(7)	100(9)	
		1009.85(15) <sup>c</sup>	0.17(3)	22(4)	
	2495.9(1) <sup>f</sup>	1706.7(1) <sup>c</sup>	1.04(13)	100(13)	
	2543.9(2) <sup>f</sup>	1754.7(2) <sup>c</sup>	0.37(6)	100(16)	
		1230.3(2) <sup>c</sup>	0.32(7)	86(19)	
	2567.5(1) <sup>f</sup>	1778.3(1) <sup>c</sup>	0.74(9)	100(12)	
	2610.7(1) <sup>f</sup>	1821.4(1) <sup>c</sup>	0.55(7)	100(13)	

<sup>a</sup>From the adopted  $\gamma$  data of Ref. [16].

<sup>b</sup>Spin assignment from angular correlation analysis.

<sup>c</sup> $\gamma$ -ray line was not previously reported.

<sup>d</sup>A level at 1384 keV was proposed in Ref. [18] based on depopulating transitions of 594.7 and 1384.0 keV. In the present work we find no evidence for these transitions; however, a 1089-keV transition in coincidence with only the 294.4-keV transition supports a level at 1384 keV.

<sup>e</sup>In Ref. [18] a 1669.4-keV level depopulated by a 1375.0-keV  $\gamma$  ray is reported while in Ref. [15] a 1671.3-keV level depopulated by a 881.9-keV  $\gamma$  ray is reported. Both  $\gamma$  rays are observed in the present work and their measured energies are consistent with a single level at 1669.7 keV.

<sup>f</sup>Level was not previously reported.

<sup>g</sup>Reported in Ref. [18] as a single depopulating transition from a level at 2232 keV. Present  $\gamma$ - $\gamma$  data indicate the 1442.8-keV line in coincidence with only the 294-keV transition.

a more  $\gamma$ -soft potential and suggesting that a first-order phase transitional description is not applicable for those nuclei in the  $N < 82$  rare-earth region.

This work was supported by the Department of Energy Office of Nuclear Physics under Contract No. DE-AC02-98CH10946 and Grant No. DE-FG02-91ER-40609.

- [1] R. F. Casten and N. V. Zamfir, *Phys. Rev. Lett.* **87**, 052503 (2001).
- [2] R. Krücken *et al.*, *Phys. Rev. Lett.* **88**, 232501 (2002).
- [3] D. Tonev, A. Dewald, T. Klug, P. Petkov, J. Jolie, A. Fitzler, O. Moller, S. Heinze, P. von Brentano, and R. F. Casten, *Phys. Rev. C* **69**, 034334 (2004).
- [4] M. A. Caprio *et al.*, *Phys. Rev. C* **66**, 054310 (2002).
- [5] F. Iachello, *Phys. Rev. Lett.* **87**, 052502 (2001).
- [6] P. E. Garrett *et al.*, *Phys. Rev. Lett.* **103**, 062501 (2009).
- [7] W. D. Kulp *et al.*, *Phys. Rev. C* **77**, 061301(R) (2008).
- [8] J. F. Sharpey-Schafer *et al.*, *Eur. Phys. J. A* **47**, 5 (2011).
- [9] C. J. Lister *et al.*, *Phys. Rev. Lett.* **55**, 810 (1985).
- [10] R. Krücken *et al.*, *Nucl. Phys. A* **589**, 475 (1995).
- [11] A. F. Mertz *et al.*, *Phys. Rev. C* **77**, 014307 (2008).
- [12] A. Gade, I. Wiedenhöver, M. Luig, A. Gelberg, H. Meise, N. Pietralla, V. Werner, and P. von Brentano, *Nucl. Phys. A* **673**, 45 (2000).
- [13] Yu. Khazov, A. A. Rodionov, S. Sakharov, and Balraj Singh, *Nucl. Data Sheets* **104**, 497 (2005).
- [14] M. Kortelahti, E. F. Zganjar, R. L. Mlekodaj, B. D. Kern, R. A. Braga, R. W. Fink, and C. P. Perez, *Z. Phys. A* **327**, 231 (1987).
- [15] M. O. Kortelahti, B. D. Kern, R. A. Braga, R. W. Fink, I. C. Girit, and R. L. Mlekodaj, *Phys. Rev. C* **42**, 1267 (1990).
- [16] A. A. Sonzogni, *Nucl. Data Sheets* **103**, 1 (2004).
- [17] A. Gizon, J. Genevey, C. F. Liang, P. Paris, D. Barnéoud, J. Inchaouh, I. Penev, and A. Plochocki, *Eur. Phys. J. A* **12**, 309 (2001).
- [18] K. S. Vierinen, J. M. Nitschke, P. A. Wilmarth, R. B. Firestone, and J. Gilat, *Nucl. Phys. A* **499**, 1 (1989).